MAGNETIZED AND FLAT BEAM EXPERIMENT AT FAST

A. Halavanau[1,2], J. Hyun[3], D. Mihalcea[1], P. Piot[1,2], T. Sen[2], C. Thangaraj[2]
[1] Department of Physics and Northern Illinois Center for Accelerator & Detector Development, Northern Illinois University DeKalb, IL 60115, USA
[2] Fermi National Accelerator Laboratory, Batavia IL 60510, USA
[3] SOKENDAI, Ibaraki, Japan

Abstract

A photocathode, immersed in solenoidal magnetic field, can produce canonical-angular-momentum (CAM) dominated or "magnetized" electron beams. Such beams have an application in electron cooling of hadron beams and can also be uncoupled to yield asymmetric-emittance ("flat") beams. In the present paper we explore the possibilities of the flat beam generation at Fermilab's Accelerator Science and Technology (FAST) facility. We present optimization of the beam flatness and four-dimensional transverse emittance and investigate the mapping and its limitations of the produced eigen-emittances to conventional emittances using a skew-quadrupole channel. Possible application of flat beams at the FAST facility are also discussed.

INTRODUCTION

A charged particle with mass m and charge q moving in axially symmetric EM-field has a constant of motion associated with its canonical angular momentum (CAM). This statement is also known as Busch's theorem and conventionally the integral of motion is written as [1]:

$$L = \gamma m r^2 \dot{\theta} + \frac{1}{2} e B_z(z) r^2 + O(r^4), \tag{1}$$

where (r, θ, z) are cylindrical coordinates.

The conservation of the CAM L yields that the mechanical angular momentum (MAM) of the beam in the magnetic-field-free zone is: $|\boldsymbol{L}| = \gamma m |\boldsymbol{r} \times \frac{d\boldsymbol{r}}{dt}| = \frac{1}{2} e B_{0z} r_0^2$, where is the field at the cathode surface, r_0 is the particle coordinate at the cathode and r is the particle coordinate at the measurement location downstream of the cathode. The norm of $|\boldsymbol{L}|$ can be computed as $L = |\boldsymbol{r} \times \boldsymbol{p}| = x p_y - y p_x$.

Following Ref. [2], we introduce the magnetization $\mathcal{L} \equiv \langle L \rangle / 2\gamma mc$, which characterizes the MAM (mechanical angular momentum) associated to the beam. Let's also define a geometric 4D emittance as $\epsilon_{4D} = \epsilon_u^2 = \sqrt{|\Sigma|} = (\sigma\sigma')^2$, where ϵ_u - uncorrelated round beam emittance, Σ is 4×4 beam matrix, and σ and σ' are respectively the round-beam RMS size and divergence. A beam is said to be magnetized when $\mathcal{L} \gg \epsilon_u$. One can show that in such a state the new eigenemittances are [3–7]:

$$\epsilon_\pm = \sqrt{\epsilon_u^2 + \mathcal{L}^2} \pm \mathcal{L} \rightarrow \epsilon_+ \approx 2\mathcal{L}; \epsilon_- \approx \frac{\epsilon_u^2}{2\mathcal{L}} \tag{2}$$

and therefore the emittance ratio or "flatness" will be:

$$\frac{\epsilon_+}{\epsilon_-} = \frac{4\mathcal{L}^2}{\epsilon_u^2} = \frac{1}{p_z^2} e^2 B_{0z}^2 \frac{\sigma_0^2}{\sigma_0'^2}$$

Previously, experimental generation of CAM and flat beams was demonstrated at Fermilab's A0 facility [8–11] and an emittance ratio of 100 was achieved at the beam energy of 15 MeV and bunch charge of 0.5 nC. The forthcoming round of experiment at IOTA/FAST facility will focus on further (*i*) understanding the round-to-flat beam transformation over various operating parameters, (*ii*) exploring the generation of compressed flat beams [12], (*iii*) investigating possible applications of the produced flat beams.

IOTA/FAST FACILITY

IOTA/FAST facility depicted on Fig. 1 is electron accelerator facility at Fermilab which will comprise of linear 300 MeV injector and 150 MeV electron ring. The injector beamline includes a L-band RF gun with a Cs:Te photocathode on its back plate. The gun is surrounded by a bucking and main solenoids, positioned in a way that they nominally yield a vanishing magnetic field B_{0z} at the photocathode surface. When the solenoids are tuned to provide a non-vanishing axial magnetic field B_{0z} at the cathode, the electrons acquire CAM (see Table 1).

Table 1: Low-energy Section Beam Parameters of the IOTA/FAST Injector

Parameter	Value	Units
Transverse emittance (norm.)	<2	μm
Beam energy	50	MeV
Slice energy spread	<5	keV
Nominal charge	200	pC
Bunch length	5	ps
Beta-function (CC2 exit)	8	m
Chicane slit mask width, w	50	μm
Energy chirp, h	-5	m^{-1}
Chicane dispersion, η	-0.3	m
Longitudinal dispersion, R_{56}	-0.18	m

Electrons are further accelerated in two 1.3 GHz SRF accelerating cavities up to the energy of 50 MeV; electron bunch can be also compressed in the magnetic chicane, located upstream of the cryomodule - a total of 8 1.3 GHz SRF accelerating cavities that boost the beam up to 300 MeV. Injector optics can be matched and loaded in the machine on-the-fly via recently developed control tools [13]. For a detailed description of the facility, please see Refs. [14–16]. IOTA/FAST injector has a number of vertical and horizontal multislit diagnostic stations located up-/downstream of

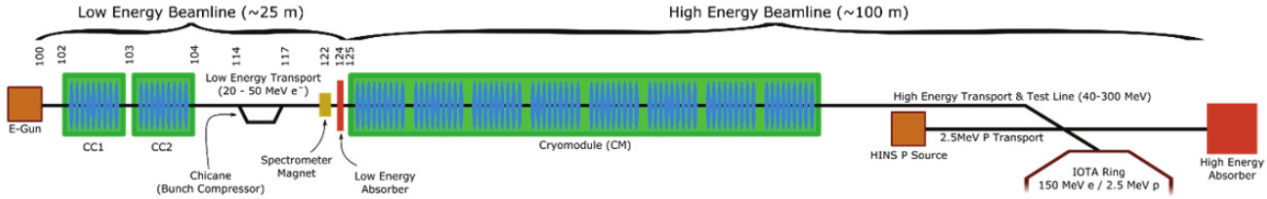

Figure 1: IOTA/FAST beamline.

the bunch compressor (at X107 and X118 locations), that allow measurement of the beam emittance in both transverse planes [17]. These devices will be used to study the conservation of ϵ_u and emittance dilution during bunch compression [12]. Furthermore, IOTA/FAST injector contains multiple YAG viewers, which can be used for quadrupole scan emittance measurement. Additional multislit mask is installed inside magnetic chicane to allow formation of the microbunched beams for further radiation generation experiments.

CAM REMOVAL

CAM can be removed from electron beam by propagating it through the series of three skewed quadrupoles. Such a quadrupole channel is conventionally called Round-to-Flat Beam (RTFB) adapter or transformer. Let the RTFB transformer be described by matrix product $R_{RTFB} = Q_3 D_3 Q_2 D_2 Q_1$, where $D_i = \begin{pmatrix} 1 & d_i \\ 0 & 1 \end{pmatrix}$ and $Q_i = \begin{pmatrix} 1 & 0 \\ \pm q_i & 1 \end{pmatrix}$ drift and quadrupole transfer matrix respectively. $R_{RTFB} = M_{-45} R'_{RTFB} M_{45}$, where M_ϕ is rotation matrix. Note, that R_{RTFB} is 4×4 matrix and D_i and Q_i are 2×2 main diagonal blocks of the 4×4 transverse transfer matrix of drift (quadrupole) respectively. Then the beam second moment matrix $\Sigma_0 = \begin{pmatrix} \Sigma_{XX} & \Sigma_{XY} \\ \Sigma_{YX} & \Sigma_{YY} \end{pmatrix}$ is transformed as $\Sigma_f = R_{RTFB} \Sigma_0 \tilde{R}_{RTFB}$, where $\Sigma_{\{X,Y\},\{X,Y\}}$ are 2×2 blocks of Σ matrix, Σ_0 is the beam matrix at the entrance of the RTFB transformer, Σ_f is the beam matrix at the exit of the transformer. RTFB transformer transfer matrix can be rewritten in block form as $R_{RTFB} = \begin{pmatrix} A & B \\ C & D \end{pmatrix}$ and the condition to remove CAM $\Sigma_{f_{XY}} = 0$ yields [18]:

$$A\Sigma_0 \tilde{B} + B\Sigma_0 \tilde{A} + A\Sigma_C \tilde{A} + B\tilde{\Sigma}_C \tilde{B} = 0.$$

Solving the latter matrix equation gives two sets of solution for quadrupole strength $q = 1/f$, where f is focal length; see also Ref. [9]

$$q_1 = \pm \sqrt{\frac{-d_2(d_T s_{21} + s_{11}) + d_T s_{22} + s_{12}}{d_2 d_T s_{12}}},$$
$$q_2 = \frac{(d_2 + d_3)(q_1 - s_{21}) - s_{11}}{d_3(d_2 q_1 s_{11} - 1)}, \quad (3)$$
$$q_3 = \frac{d_2(q_2 - q_1 q_2 s_{12}) - s_{22}}{d_2(d_3 q_2 s_{22} + q_1 s_{12} - 1) + d_3(s_{12}(q_1 + q_2) - 1)},$$

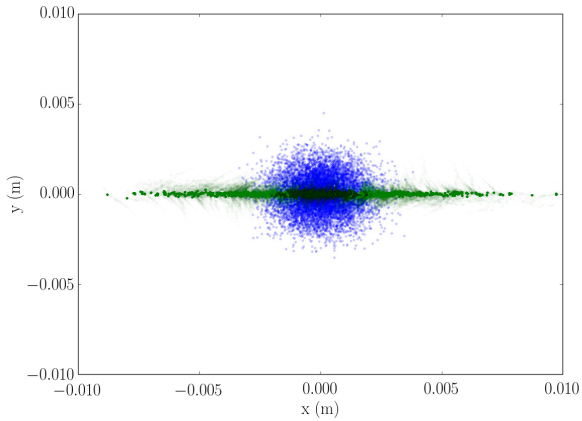

Figure 2: Demonstration of CAM removal in ELEGANT simulations for the case of $\epsilon_u = 2$ μm and $\epsilon_+/\epsilon_- = 400$.

Table 2: Comparison between linear approximation from Eq. 3 and ELEGANT simplex optimization

Model	q_1, m^{-1}	q_2, m^{-1}	q_3, m^{-1}
Linear model	1.84	-1.2	0.23
Elegant simplex (1000 p.)	1.88	-1.39	0.20

where q_i is the quadrupole strength, d_2, d_3 are the distances between first and second, and second and third quadrupole respectively, s_{ij} are the elements of 2×2 matrix S that is defined as [2]: $S = \pm \frac{1}{|\Sigma_{0_{XX}}|} J \Sigma^{-1}_{0_{XX}} = \mp \frac{1}{\epsilon} \begin{pmatrix} 0 & -\sigma^2 \\ \kappa^2\sigma^2 + \sigma'^2 & 0 \end{pmatrix}$, where $\kappa = \mathcal{L}/\sigma^2$, $\Sigma_{0_{XX}}$ is 2×2 block of beam matrix, J is symplectic unit matrix and $\epsilon = \sqrt{\epsilon_u^2 + \mathcal{L}^2}$. For simplicity of the derivation, it was assumed the beam has a waist at the entrance of the RTFB transformer.

For IOTA/FAST quadrupole magnet the following relation is used to calculate it's current: $I_q = (1.8205K \times p\,[MeV/c])/405.4$, where $K = q/L_{eff}$ and $L_{eff} = 16.7cm$ is the effective length of the quadrupole.

BEAM DYNAMICS SIMULATIONS

In order to investigate beam dynamics associated to non-zero residual magnetic field at the photocathode, we implemented IOTA/FAST injector beamline model in several codes: ASTRA, IMPACT-T and ELEGANT [19–21]. First, RF-gun solenoids configuration was optimized in ASTRA. The

ISBN 978-3-95450-182-3

maximum B_z field at the cathode is 0.2 Tesla, and with bucking solenoid not reversed it is 0.18 Tesla. To ensure appropriate beam dynamics (e.g. no particle loss, good emittance, etc.) a comprehensive multi-objective genetic algorithm optimization was performed using the code [22] and IMPACT-T low energy beamline model. During the optimization, the Pareto fronts for bunch charge $Q = 1, 20, 200$ pC and ϵ_u were determined, and configurations with $\epsilon_u < 2\mu$m were selected for further study. Figure 3 represents simulated spot size as a function of $\mathcal{L}$ and laser spot size on the cathode. To simulate beam dynamics in magnetic chicane, IMPACT-T model was used. Total energy spread was found to be 0.088% with uncorrelated energy spread at the center of the bunch 0.32 keV.

EXPERIMENTAL PLAN FOR RUN 2017

Prior to implementation of the RTFB transformer, an optimization of the round electron beam is required. For that matter, multislit emittance stations and quadrupole scan technique will be used. The initial values of the RTFB transformer settings will be calculated via Eq.3, then ELEGANT simplex optimization will be used to correct for chromaticity and other second order effects in the magnets; see Table 2 for example comparison. The RTFB adapter performance will be first demonstrated with low B_{0z} value and then further optimized for maximum flatness. Beams with flatness of 400 and $\epsilon_- = 20$ nm are expected at Q=200 pC; see Fig. 2. A dedicated study will be performed for the case of $Q = 2.2$ nC as a particular interest and possible future applications of magnetized beams in Jefferson Lab Electron-Ion Collider (JLEIC) project.

THZ RADIATION GENERATION

Multislit mask inserted in the magnetic chicane impose energy modulation which will be converted into density modulation upon the exit of the chicane. Such mechanism can be used for microbunching generation and further radiation generation. The radiation spectrum of the electron bunch is given by:

$$\left(\frac{d^2W}{d\mathbf{k}d\Omega}\right)_{total} = [N + N(N-1)b(\mathbf{k})^2]\left(\frac{d^2W}{d\mathbf{k}d\Omega}\right)_e,$$

where $\left(\frac{dW}{d\mathbf{k}d\Omega}\right)_e$ represents the single-electron radiation spectral fluence associated to the considered electromagnetic process (coherent transition radiation, CTR), $b(\mathbf{k}) = \int \rho(x,y,z)\exp\left[-i(k_x x + k_y y + k_z z)\right]dxdydz$ is the bunch form factor and $\rho(x,y,z)$ is the bunch distribution. In order for CTR spectrum to be independent of transverse beam size σ_r, it has to satisfy $\frac{1}{2}(k_x^2 + k_y^2)\sigma_r^2 << 1$ and $\sigma_r < 6.7$ mm at the radiator for 50MeV beam at frequency of radiation of 1 Thz. At the exit of the chicane, the bunch length is described by $\sigma_z = \frac{1}{\eta h}\sqrt{\eta^2\sigma_u^2 + (1 + hR_{56})^2(\Delta X^2 + \epsilon\beta)}$, where $\eta = -0.3$m is chicane dispersion, h is the energy chirp, σ_u is relative beam energy spread, $\Delta X = w/(2\sqrt{3})$ - RMS width of the slits, ϵ - geometric emittance and β is beta-function

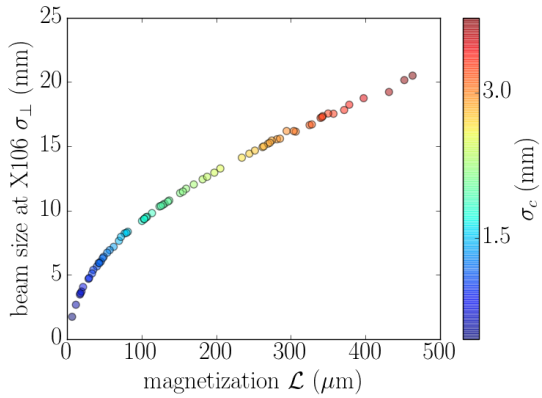

Figure 3: Beam size at the first skew quadrupole entrance as a function of $\mathcal{L}$ and laser spot size on the cathode.

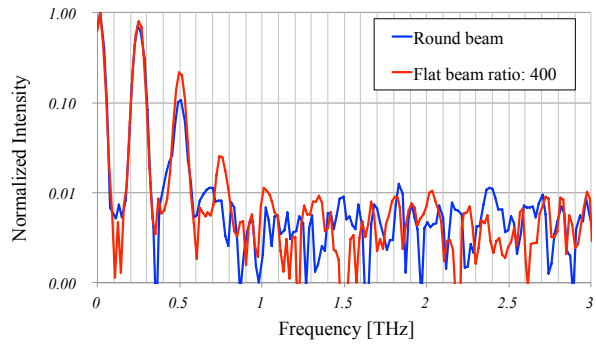

Figure 4: Enhancement of the radiation spectrum represented in THz frequency domain for the case of round and flat beam depicted on Fig. 2.

value at the mask. When incorporated into Gaussian beam distribution $\rho(x,y,z)$, reduction of the geometric emittance can improve the peaks intensity of the radiation.

Using ELEGANT, the optics is matched so that the $\beta_x = 0.5$m at the slit (beam waist). with the five quadrupoles upstream of the chicane. The transmission rate of the electrons passing through the slits was about 5 % from particle tracking. The microbunched electron beam distribution along the longitudinal direction is obtained after the chicane and plotted in Fourier domain on Figure 4, therefore represents the expected radiation spectra for the round beam and the flat beams. A dominant factor is the slice energy spread, which, if reduced, can further significantly increase the intensity of the radiation spectrum. Spectra displayed on Fig. 4 will be experimentally measured with a Martin-Puplett interferometer equipped with two pyroelectric detectors

CONCLUSIONS

IOTA/FAST injector is capable of producing strong CAM modulated beams that can be used for various beam physics studies. Additionally, THz radiation generation process in the magnetic chicane can be enhanced by using emittance partitioning technique in RTFB transformer.

REFERENCES

[1] M. Reiser. *Theory and design of charged particle beams* (1995).

[2] K. J. Kim. *Phys. Rev. ST Accel. Beams*, 6:104002, (2003).

[3] Ya. Derbenev. Adapting optics for high-energy electron cooling, UM-HE-98-04-A, (1998).

[4] K. Kubo. *ATF Internal Report, ATF-99-02* (1999).

[5] R. Brinkmann, Ya. Derbenev, and K. Flottmann. *Phys. Rev. ST Accel. Beams*, **4**, 053501 (2001).

[6] S. Nagaitsev and A. Shemyakin, FERMILAB-TM-2107, (2000).

[7] S. Lidia. *LUX Tech Note-012, LBNL-56558* (2012).

[8] D. Edwards, *et al*, *Proc. of LINAC2000*, paper MOB13, (2000).

[9] E. Thrane, *et al*, *Proc. of LINAC2002*, paper TU404, (2002).

[10] Y. E Sun, P. Piot, K. J. Kim, N. Barov, S. Lidia, J. Santucci, R. Tikhoplav, and J. Wennerberg. *Phys. Rev. ST Accel. Beams*, **7**, 123501 (2004).

[11] P. Piot and Y. E. Sun, *FERMILAB-CONF-14-142-APC* (2014).

[12] J. Zhu, P. Piot, D. Mihalcea, and C. R. Prokop. *Phys. Rev. ST Accel. Beams*, **17**, 084401 (2014).

[13] P. Piot and A. Halavanau, *FERMILAB-CONF-16-464-AD-APC*, (2016).

[14] S. Antipov, *et al*, *Journal of Instrumentation*, 12(03):T03002, (2017).

[15] E. Harms, *et al*, *ICFA Beam Dyn.Newslett.*, 64:133–156, (2014).

[16] P. Piot, *et al*, Beam dynamics simulations of the nml photoinjector at fermilab. *Proc. of IPAC'10*, (2010). Kyoto, Japan, 4316.

[17] Min Zhang. Emittance formula for slits and pepper pot measurement. (1996).

[18] Karl L. Brown. *Adv. Part. Phys.*, 1:71–134, (1968).

[19] J, Qiang *IMPACT-T reference manual*, LBNL-62326, (2007).

[20] K. Flöttmann. *ASTRA reference manual*, DESY (2000).

[21] M. Borland. *Advanced Photon Source*, LS-287, (2000).

[22] H. Shang. Multi-object geneticoptimizer and its application. *OAG-TN-2007-028*, (2007).

ISBN 978-3-95450-182-3